Reference crop evapotranspiration database in Spain (1961-2014)

Miquel Tomas-Burguera[1], Sergio M. Vicente-Serrano[2], Santiago Beguería[1], Fergus Reig[2], and Borja Latorre[1]

[1]Estación Experimental de Aula Dei, Consejo Superior de Investigaciones Científicas (EEAD-CSIC), Avda. Montañana 1005, Zaragoza, E-50059, Spain
[2]Instituto Pirenáico de Ecología, Consejo Superior de Investigaciones Científicas (IPE-CSIC), Avda. Montañana 1005, Zaragoza, E-50059, Spain

Correspondence: Miquel Tomas-Burguera (mtomas@eead.csic.es)

Abstract.

Obtaining climate grids for distinct variables is of high importance to develop better climate studies, but also to offer usable products for other researchers and to end users. As a measure of atmospheric evaporative demand (AED), reference evapotranspiration (ET_o) is a key variable for understanding both water and energy terrestrial balances, being important for climatology,

5   hydrology and agronomy. In spite of its importance, the calculation of ET_o is not very common, mainly because data of a high number of climate variables are required, and some of them are not commonly available.

To solve this problem, a strategy based on the spatial interpolation of climate variables previous to calculation of ET_o using FAO-56 Penman-Monteith was followed to obtain an ET_o database for Continental Spain and Balearic Islands covering the 1961-2014 period at a spatial resolution of 1.1 km and at weekly temporal resolution. In this database, values for the radiative

10   and aerodynamic components as well as the estimated uncertainty related with ET_o are also provided.

This database is available to download in Network Common Data Form (netcdf) at http://dx.doi.org/10.20350/digitalCSIC/8615 (Tomas-Burguera et al., 2019), and a map visualization tool (http://speto.csic.es) is also available to help users to download data of one specific point in comma-separated values (csv) format.

A relevant number of research ares could take advantage of this database. Providing only some examples: i) the study of

15   budyko curve, which relates rainfall data with evapotranspiration and AED at watershed scale; ii) the calculation of drought indices using AED data, such as SPEI or PDSI; iii) agroclimatic studies related with irrigation requirement; iv) validation of Climate Models water and energy balance; v) the study of the impacts of climate change in AED.

1   Introduction

20   As a measure of atmospheric evaporative demand (AED), reference evapotranspiration (ET_o) is a key variable for understanding both water and energy terrestrial balances, being important for climatology, hydrology and agronomy (Espadafor et al., 2011).

To compute ET_o, the Food and Agriculture Organization of the United Nations (FAO) recommends the use of a modified version of Penman-Monteith (Allen et al., 1998), requiring data of maximum and minimum air temperature, air humidity, wind speed and solar radiation. While maximum and minimum air temperature are commonly collected at weather observatories, the observation of the rest of variables is scarce, specially if long time series are required for climate studies (McVicar et al.,

5   2007; Irmak et al., 2012).

Main problems affecting the generation of ET_o climate grids are related to climate data availability: a) some of the variables needed to compute ET_o are not commonly available (Vanderlinden et al., 2004; Vicente-Serrano et al., 2014) and b) changes in observation network difficult the generation of climate grids as the use of a changing number of observations can introduce non climatic changes in variance (Beguería et al., 2016).

10   When some of the variables are not commonly available, possible solutions that allow ET_o calculation can be classified in two groups: i) use of less demanding methods and ii) estimation of missing data previous to ET_o calculation.

i) Less demanding methods

The use of less demanding methods, such as Thornthwaite (Thornthwaite, 1948) or Hargreaves and Samani (1985), is still very common, specially because temperature is commonly available and temperature and solar radiation accounts for 80 % of

15   the ET_o variability (Mendicino and Senatore, 2013; Samani, 2000). Nevertheless, this strategy is not recommended as methods not using data for all climatic variables are not able to deal with the variability and/or trends of missing variables and they could lead to erroneous conclusions (Irmak et al., 2012; Mcvicar et al., 2012; Sheffield et al., 2012; Tomas-Burguera et al., 2017).

ii) Estimation of missing data

20   The estimation of missing data previous to ET_o calculation can also be divided in two possibilities: i) the use of FAO-56 recommendations and ii) the use of nearby weather stations data. Whenever data of the non-observed variable exist at nearby locations, the use of FAO-56 recommendations should be avoided because: a) they use stationary relationships between variables, leading to similar problems than those detected for less demanding methods (Tomas-Burguera et al., 2017) and b) data of temperature is always required.

25   The use of nearby weather stations data to estimate missing data takes advantage of spatial interpolation methods, and it is the only of the above mentioned methods that estimate the missing data using information of the same variable. This strategy, usually known as Interpolate-then-Calculate (IC), has two main steps. First, the missing variables are estimated using a spatial interpolation method and then, Penman-Monteith is calculated. This method was tested in various regions, such as Greece, China, Great Britain (Mardikis et al., 2005; McVicar et al., 2007; Robinson et al., 2017). Tomas-Burguera et al. (2017), in the

30   Iberian Peninsula, compared the performance of this method with some of the aforementioned solutions, concluding that IC strategy was the one obtaining better results.

The other problem related with data availability is that climatic networks changes over time, affecting the number of available observations.

In Spain, relevant changes affected the availability of wind speed and relative humidity data during last decades, as the

35   installation of a high number of automatic weather stations (AWS) 10 years ago implied a sharply increase in data availability

of these relevant variables for ET_o calculation. Nevertheless, and as it was mentioned before, it is important to use a constant number of observations through time when a climate grid wants to be generated by using a geostatistical method, such as universal kriging. That means that only the longest climate time series should be used to generate the climate grids, diminishing the number of weather observations that can be used. In order to extend the number of observations, it is common to use a gap filling procedure, which estimate the missing data from one specific weather station using as a reference the data from nearby well-correlated time series.

This research is focused on the generation of a climate grid of ET_o for Continental Spain and Balearic Islands with a spatial resolution of 1.1 km covering the 1961-2014 period with a weekly temporal resolution. The followed methodology, which mainly consists in the combination of two estimation processes to overcome the above mentioned problems previous to ET_o calculation is presented in this paper. A gap filling procedure was used to obtain a subset of complete time series for the period of interest for each one of the climatic variables, and a spatial interpolation methodology was implemented to generate climate grids of each one of the required climate variables previous to the calculation of ET_o, meaning that a PM-IC scheme was implemented. Quality control and homogenization steps were also implemented. The validation of gap filling, homogenization and interpolation steps are presented trying to detect possible spatial or temporal effects that could affect to ET_o obtained values.

Although it is not commonly implemented, an uncertainty propagation scheme was also implemented, considering the two estimation processes (gap filling and interpolation) as the unique sources of uncertainty.

2 Data sources

The original dataset contains data of daily maximum temperature (Tmax), minimum temperature (Tmin), wind speed (W), relative humidity (RH) and sunshine duration (SD) provided by AEMET for the whole Spain. Sunshine duration is used to estimate radiation data as the number of weather stations collecting radiation data is very low and Sanchez-Lorenzo et al. (2013) obtained a good adjustment between these two variables.

The number of observations available (Table 1) depends on the variable. More than 4000 weather stations are available both for maximum and minimum temperature. Less than 1000 weather stations are available for the others variables, being less than 300 for sunshine duration. The number of selected weather stations is always much lower than the available ones, as only the longest time series were selected.

These weather stations did not collect data throughout the entire period. Figure 1 shows, for each variable and each year, the number of weather observations available for the 1961-2014 period. Temperature data show the highest number of observations, always higher than 500, reaching 2000 observations available in the mid 90's with a posterior decrease. Relative humidity and wind speed show a low number of observations during the study period. Nevertheless, in the mid 2000's, when the installation of a high number of automatic weather stations (AWS) took place, a sharply increase in the availability of these two climatic variables is detected. Sunshine duration measurements are constant throughout the whole period

Some geographic variables were also used in the interpolation process. Digital Elevation Model (DEM) was obtained from the IGN (Instituto Geográfico Nacional), and other variables, such as distance to the sea, were derived from the DEM.

3   Methodology

The general scheme to generate the ET_o database has two main steps: i) generation of climatic grids and ii) estimation of ET_o
5   (Figure 2). The generation of the climatic grids can be divided in: a) daily quality control, b) daily to weekly data conversion, c) gap filling, d) data selection, e) homogenization and f) interpolation and all of these steps are implemented individually for each climatic variable. The estimation of ET_o consists in the calculation of ET_o by using the FAO-56 Penman-Monteith equation using the climatic grids as the source of data.

On the other hand, the uncertainty of ET_o was also estimated using a two steps process: i) uncertainty estimation of climatic
10 grids and ii) uncertainty propagation from climatic grids to ET_o. The uncertainty estimation of climatic grids refers to the uncertainty of each climatic grid after the interpolation process and it takes into account the uncertainty related both with the gap filling process and with the interpolation process. The uncertainty propagation refers to the technique that estimates the uncertainty of ET_o values by combining the uncertainty of each climatic variable with the Jacobian of the Penman-Monteith equation.

15 The daily quality control was implemented in R and, for each variable, all data available was evaluated at time. The tests at daily time scale are based on the detection of erroneous codificated and abnormal values (Tomas-Burguera et al., 2016).

Then, daily data was converted to weekly data. Trying to adapt the WMO rules for monthly data (WMO, 1989) to weekly data, those weeks with at least two missing values are considered to have no value.

Some comparison problems between distinct years emerge when time scale of 7 days is used, mainly because number of
20 days in a year is not divisible per 7. Trying to combine the weekly time scale with comparability between distinc years, each month was divided in 4 periods (days 1-8, 9-15, 16-22, 23-end). From now on, the use of word weeks in this paper refers to this definition of sub-monthly period.

After this step, relative humidity data was transformed into dewpoint temperature (T_d) using also temperature data. After some tests with gap filling and interpolation, it was noticed that working with T_d was easier than working with RH. As T_d data
25 adjust better to a gaussian distribution than RH data, working with T_d data is preferrable in most of the implemented steps.

3.1   Gap filling

Trying to obtain complete time series of distinct climate variables, a gap filling procedure based on the estimation of missing data by using nearby weather stations' data designed by (Beguería et al., 2019) was implemented. The standard error of the estimated data was also obtained and used as a measure of the uncertainty of the process.

30 The selecion of used nearby weather stations is relevant for the process, and a selection based on three steps was implemented: i) overlapping period higher than 7 years; ii) location closer than 100 km and iii) values of R^2 higher than 0.6.

The used procedure uses standardization of values previous to the gap filling, in order to avoid problems related with differences in the mean values and/or in the variance between weather stations.

The gap filling was implemented individually for each climatic variable and more than one (3) gap filling loop was implemented for less frequent variables (sunshine duration, dewpoint temperature and wind speed). The use of various steps in the gap filling procedure was implemented to take advantage of non-overlapping data, and it was used previously to generate other databases in Spain (Gonzalez-Hidalgo et al., 2015).

A high number of complete time series for each variable was obtained after this process, but only time series containing a high percentage of original data was selected to be used in the interpolation process. For temperature, only time series accounting for more than 25 years of original data were used. For the rest of variables, this period was reduced to 15 years, due to the low availability of long records (Figure 3).

3.2 Homogenization

To test the homogeneity of the obtained time series after the gap filling process we used the Standard Normal Homogeneity Test (SNHT) (Alexandersson, 1986). The test was implemented at monthly time scale after the conversion of time series to this time scales, mainly because homogeneity tests, in general, are more robust when they are used with monthly data than with sub-monthly. In order to obtain weekly homogeneous time series, once the monthly parameters are obtained we transformed to weekly parameters.

The homogenization of the climate series was tested after the gap filling due to: i) it is possible to detect inhomogeneities introduced by the gap filling process and ii) the process is more reliable when time series have no gaps.

Present observations were assumed to be the standard, meaning that in case of detecting any inhomogeneity, the correction was made to adjust the values of the past to the present values.

3.3 Interpolation

Kriging is a geostatistical method widely used in Climatology to generate interpolated surfaces for many variables (Aalto et al., 2013; Hofstra et al., 2008). Kriging is, in fact, a set of different methods such as ordinary kriging (OK) or Universal Kriging (UK). The main difference between OK and UK is that the former assumes the presence of a spatial constant mean, while the latter assumes the spatial mean is a function that can depend on geographical factors (Cressie, 1993). The last assumption is preferrable in Climatology, at climate variables commonly varies depending on geographical factors such as latitude, longitude or elevation (Aalto et al., 2013). In this paper, climate grids for each varieable were generated individually by using UK to predict a value at each grid point of interest for each time step.

One interpolation process was executed for each variable and for each time step. Previous to the interpolation, a semivariogram model was generated, being unique for each time step and each climatic variable. This process was implemented using the gstat package in R (Pebesma, 2004; Gräler et al., 2016).

Using universal kriging a variance of the prediction was also obtained, and this value was used as an estimator of the uncertainty. One of the advantages of using gstat package is that an uncertainty associated with observed data can be provided.

At this point, we decided to use the quantification of the uncertainty obtained from the gap filling process, which is the previous estimation process.

3.4 ET$_o$ calculation

Predicted values of distinct climate variables were used to calculate ET$_o$ by using the FAO-PM equation (Allen et al., 1998).

$$\text{ET}_o = \frac{0.408\,\Delta\,(R_n - G) + \gamma\,(\frac{900}{T+273})\,U_2\,(e_s - e_a)}{\Delta + \gamma\,(1 + 0.34\,U_2)} \tag{1}$$

where R_n is the net radiation at the crop surface ($MJ\,m^{-2}day^{-1}$), G is the soil heat flux density ($MJ\,m^{-2}day^{-1}$), T is the mean air temperature at 2 m (°C), U_2 is the wind speed at 2 m (ms^{-1}), e_s is the saturation vapor pressure (kPa), e_a is the actual vapor pressure (kPa), $e_s - e_a$ is the saturation vapor pressure deficit (kPa), Δ is the slope of the vapor pressure curve ($kPa\,°C^{-1}$) and γ is the psychrometric constant ($kPa\,°C^{-1}$). The value 0.408 is used to convert from $MJ\,m^{-2}day^{-1}$ units
10 to $kg\,m^{-2}day^{-1}$ (alternatively: $mm\,day^{-1}$).

Following recommendations of Allen et al. (1998), we fixed G to 0 as we estimated ET$_o$ for a time period lower than 10 days.

The main advantage of this equation is that it is physically-based and it accounts for both the radiative and aerodynamic components of evapotranspiration, being the former related to the available energy for evaporation and the latter related to the
15 capacity of the air to store the vapor from evapotranspiration (Azorin-Molina et al., 2015). While the radiative component is strongly related to the solar radiation, hence presenting a high seasonality in the study region due to its latitude, the aerodynamic component is more variable throughout the year as it is influenced by the vapor pressure deficit but also by the wind speed. If Eq. (1) is splitted in the summation of its two parts, one part could be interpreted as the radiative component (ET$_{oRa}$) and the other part as the aerodynamic component (ET$_{oAe}$).

$$\text{ET}_{oRa} = \frac{0.408\,\Delta\,(R_n - G)}{\Delta + \gamma\,(1 + 0.34\,U_2)}$$

$$\text{ET}_{oAe} = \frac{\gamma\,(\frac{900}{T+273})\,U_2\,(e_s - e_a)}{\Delta + \gamma\,(1 + 0.34\,U_2)} \tag{2}$$

This dataset contains data of the two components ET$_{oRa}$, ET$_{oAe}$ and of the final value of their summation, which is ET$_o$.

3.5 ET$_o$ uncertainty estimation

ET$_o$ uncertaitny estimation has two main steps: i) uncertainty estimation of climatic grids and ii) uncertainty propagation from climatic grids to ET$_o$. Due to the complexity of the proccess of uncertainty estimation of ET$_o$, in this first version of the dataset
25 the uncertainty estimation is only provided for the final value of ET$_o$, but not for its two components (ET$_{oRa}$ and ET$_{oAe}$)

3.5.1 Uncertainty estimation of climatic grids

When climate grids are generated many uncertainty sources of data exist (uncertainty related to the observation, uncertainty related to interpolation process,...) (Haylock et al., 2008). In this paper we assumed uncertainty was only related to estimation processes, i.e. gap filling and interpolation. Moreover, we considered the uncertainty of each climatic grid at each time step is

5   equal to the uncertainty after the interpolation process.

Uncertainty estimation of the gap filling was based on the number of weather observations used to estimate the missing data and the covariance between these data. The less covariance between the data, the more uncertainty we considered.

In the interpolation process it was assumed that uncertainty was equal to the variance of the prediction, i.e. the variance of the kriging. To propagate the uncertainty estimated in the gap filling process to the interpolation process, the gstat package in

10 R was used, as it is possible to provide the uncertainty related to the observational data that will be used in the interpolation process.

3.5.2 Uncertainty propagation

The uncertainty propagation allow us to obtain the uncertainty of predicted ET_o (R) by using the posterior variance of climate grids and the Jacobian of FAO-PM.

15 $$R = J_{ETo} Q (J_{ETo})^T \tag{3}$$

where J_{ETo} is the Jacobian of ET_o and Q is the covariance matrix of variables, in which we considered (for simplicity) independence between variables, reaching to a diagonal matrix with only variance positions distinct to 0.

The Jacobian has the following form, and it was analytically derived.

$$J_{ETo} = \left[\begin{array}{ccccc} \frac{dET_o}{dT_{max}} & \frac{dET_o}{dT_{min}} & \frac{dET_o}{dTd} & \frac{dET_o}{dW} & \frac{dET_o}{dSD} \end{array} \right]$$

20 and the covariance matrix as.

$$\mathbf{Q} = \begin{bmatrix} \sigma_{T_{max}}^2 & 0 & 0 & 0 & 0 \\ 0 & \sigma_{T_{min}}^2 & 0 & 0 & 0 \\ 0 & 0 & \sigma_{T_d}^2 & 0 & 0 \\ 0 & 0 & 0 & \sigma_W^2 & 0 \\ 0 & 0 & 0 & 0 & \sigma_{SD}^2 \end{bmatrix}$$

where σ^2 is the variance of the kriging of each of the climatic variables. In fact, as Q is a diagonal matrix, the R calculation can be rewritten as:

$$R = \left(\frac{\partial ET_o}{\partial T_{max}} \right)^2 * \sigma_{Tmax}^2 + \left(\frac{\partial ET_o}{\partial T_{min}} \right)^2 * \sigma_{Tmin}^2 + \left(\frac{\partial ET_o}{\partial T_d} \right)^2 * \sigma_{Td}^2 + \left(\frac{\partial ET_o}{\partial W} \right)^2 * \sigma_W^2 + \left(\frac{\partial ET_o}{\partial SD} \right)^2 * \sigma_{SD}^2 \tag{4}$$

3.6 Using 2010-2014 data to validate air humidity and wind speed grids

In the last part of the period a high number of AWS were installed, and available data for the period 2010-2014 show a sharp increase for RH and W when compared with the available weather stations to generate the original database (Table 2).

As the climatic grid have a spatial resolution of 1.1 km a direct comparison of the estimation of climatic grid against the observed value was implemented. For the 2010-2014 period this methodology was followed to evaluate the quality of relative humidity and wind speed estimations of the climatic grid.

4 Validation

4.1 Gap filling

As the number of original data changes over time, the number of filled data also shows a temporal evolution. Figure 4 represents this temporal evolution, with a higher number of filled data during the first years of the period, with an important decline throughout the time. Nevertheless, for maximum and minimum temperature, the number of filled data increased again during the last years because a slow decline in the number of observation and the disappearance of some of the weather stations with longer records. Wind speed is the variable showing a lower percentage of filled data. Due to the high variability, both spatial and temporal, and the low number of observations available of this variable, it was difficult to obtain highly correlated time series to fill the gaps.

To verify the performance of the gap filling a comparison between original data and estimated data was developed. Evidently, this comparison was only possible for periods having original data.

In Table 3 some statistics of the process are provided. In general, the adjustment in terms of R^2 is quite good, with values higher than 0.9 for all variables except for wind speed, which shows an adjustment of only 0.53. Evaluation of ME and PBIAS show no bias for maximum and minimum temperature, a small negative bias for dewpoint temperature (-0.01 of ME and -0.15 of PBIAS) and for sunshine duration (-0.01 of ME and -0.23 of PBIAS), and a positive bias for wind speed (0.08 of ME and 0.64 of PBIAS). Ratio of mean values and ratio of standard deviation show values close to 1 for all variables. Wind speed shows a ratio of standard deviation of 1.05 meaning that the temporal variability of gap filling data is slightly higher than the temporal variability of original data.

In Figure 5 the possible existence of temporal differences in the performance of the gap filling process was evaluated by using decadal values of R^2. In general, all the analyzed periods show a similar performance. For wind speed, it seems that the most recent period show a small better performance than the rest of the period, but being for all the periods the variable showing the lower performance.

4.2 Homogenization

Statistics of data affected by homogenization process show a percentage higher than 10 % for all variables except for wind speed (Table 4). For all the variables, the percentage of homogenized is higher for filled data than for original data, showing the

importance of implementing the homogenization process after the gap filling. Two factors could explain this: i) as original data was not homogenized previous to the gap filling, the existence of inhomogeneities in original data propagates to homogenized data and ii) the possible introduction of inhomogeneities by the gap filling procedure.

The homogenization process affected specially the first decades of the study period, showing for all the variables a clear decline through time reaching values close to 0 during last years of the study period (Figure 4). This result is related with the fact that in this homogenization process, the more recent conditions were considered the standard ones.

A possible effect of this consideration is the propagation of current conditions to the past, which was evaluated by comparing the spatial mean values of homogenized and previous to homogenization time series. The Figure 6 shows the presence of this effect in the implemented homogenization process, as variables affected by a well-known positive trend, maximum and minimum temperature (del Río et al., 2012; Gonzalez-Hidalgo et al., 2016), show a positive bias in homogenized data during the first decades, and wind speed, variable affected by a negative trend (Azorin-Molina et al., 2014), shows a negative bias.

To investigate the effect of homogenization process in ET_o, a similar procedure was followed calculating the mean regional values of ET_o before and after the homogenization of the climatic variables. These regional values were obtained by calculating first a mean regional value of climatic variables and then calculating the ET_o by using the Penman-Monteith equation.

No important differences were detected when the two time series of ET_o were compared (Fig. 7). This result is relevant, as it shows that the non-desired detrending introduced by the homogenization process have no effects for the spatial mean values of ET_o.

4.3 Interpolation validation

To validate the interpolation process, a leave-one-out-cross-validation (LOO-CV) process was executed and validation statistics were calculated to evaluate the perfomance of the interpolation predicting both the temporal variability and the spatial variability. A LOO-CV process consists in the repetition of the interpolation process n-times (being n the number of observations available) using each time n-1 observations and using the predicted value at non used observatory as a way to evaluate the quality of the interpolation.

The temporal variability was evaluated by calculating the temporal statistics individually for each observatory and then computing the mean of all observatories. However, the spatial variability was evaluated by calculating the statistics at each time step using information of all observatories and then computing the mean of all time steps. The problem with LOO-CV is that validation can only be estimated at places were observations used in the interpolation process exist.

Another option to validate the interpolation process consists in the comparison of non-used observational data for the 2010-2014 period (when a high number of wind speed and relative humidity observations exist) against the interpolated values.

4.3.1 Spatial and temporal validation using LOO-CV

Statistics referring to the ability of interpolation process to predict the spatial and the temporal variability of climatic grids appears in Table 5. In general, temporal validation shows better statistics than spatial validation. In terms of R^2 all the variables, except wind speed, show values greater than 0.9 for temporal validation and close to 0.8 for spatial validation.

According to ME and PBIAS the only variable showing the presence of a bias, for both validations, is the wind speed, with a PBIAS reaching 12.31 for the temporal validation.

A temporal analysis of R^2 of the spatial validation (Fig. 8) show some differences between decades of maximum and minimum temperature, reaching the recent decades greater values of R^2 . Nevertheless, the most relevant detected effect is

5 the presence of seasonality in the R^2 of dewpoint temperature, showing lower values during summer than in winter. A higher spatial variability of air humidity in summer months due to the contrast between high air humidity at coastal areas and low air humidity at continental areas could be the reason of the presence of lower values during summer.

4.3.2 2010-2014 validation

When 2010-2014 independent time series of wind speed and relative humidity was used to validate the performance of in-

10 terpolation, the two most relevant detected problems are an overestimation of the wind speed during winter months at the northeastern region of the Iberian Peninsula and an overestimation of dewpoint temperature at inner region of the Iberian Peninsula during summer months at the same time that an underestimation was detected at maritime region. These two effects can be visualized in Figure 9, in which the mean error for January and for July for the two variables were represented.

4.3.3 Uncertainty validation

15 Data of 2010-2014 period could also be used to validate the uncertainty estimation of climatic grids. First, the Mean Absolute Error (MAE) was calculated by comparing the independent weather stations data against the climatic grid data. Then, the obtained values of MAE were compared against the uncertainty values of the climatic grids.

The mean spatial values of MAE and uncertainty are represented in the Figure 10. In general, the uncertainty of climatic grids is well estimated, specially for wind speed and for sunshine duration, variables showing similar values of MAE and

20 uncertainty. The rest of the variables (T_{max}, T_{min} and T_d) show slightly higher values of uncertainty than MAE values but always with similar temporal oscillations.

5 Discussion and conclusions

We proposed a methodology to obtain a 1961-2014 ET_o climate grid in Spain based on Penman-Monteith equation. While previous studies of ET_o and AED climatology exist in Spain (Azorin-Molina et al., 2015; Sanchez-Lorenzo et al., 2014;

25 Vicente-Serrano et al., 2014), this is the first suitable ET_o database for climate studies covering all the study area with high spatial resolution and for a long time period. High spatial resolution climate data sets of ET_o are not usually available, specially if they are developed using Penman-Monteith equation. During last years, ET_o climate grid at 1 km of spatial resolution was presented in Great Britain Robinson et al. (2017). Haslinger and Bartsch (2016) presented also a climate grid at 1 km of spatial resolution for Austria, but based on the Hargreaves equation.

30 As the number of weather stations collecting all variables required to calculate ET_o is very low, the proposed methodology takes advantage of two estimation processes, gap filling and spatial interpolation. The performance of each one of these two

steps was carefully studied trying to detect possible negative impacts in the generation of the ET_o database. In general, no relevant problems were detected for most of the climatic variables but for wind speed, which is the variable showing the worst performance in each of the estimation processes, due to its high spatial and temporal variability.

The PM-IC strategy, which is based in first interpolate the climatic variables and then calculate ET_o, was previously used in
5   other regions (Mardikis et al., 2005; McVicar et al., 2007) and determined to be the best method to estimate ET_o in scenarios of missing data in Spain (Tomas-Burguera et al., 2017). Another strategy, known as PM-CI, which is based in first calculate ET_o and then interpolate the obtained values, could also be used. The main advantage of PM-CI against PM-IC is that only one interpolation is required, but the main disadvantage is that a lot of data is misused. In the case of Spain, the use of PM-CI would restrict the calculation of ET_o to nearly 50 weather stations, which is the number of weather stations used in previous
10 studies (Vicente-Serrano et al., 2014). On the other hand, the use of PM-IC allow the use of more data, specially of temperature data, reaching more than 1000 weather stations. Considering that according to (Mendicino and Senatore, 2013; Samani, 2000), 80 % of ET_o variability is related with variability in temperature and radiation, this is relevant.

A comparison against an independent subset of climatic data for the 2010-2014 period showed the presence of a positive bias for wind speed in winter in the northeastern region of the Iberian Peninsula. This overestimation of wind speed in this region
15 can be explained by the fact that a low number of observations are used in that region, and most of the used observations are located in places affected by tramontana events. Fortunately, the higher bias is detected in winter, when ET_o values are lower and the importance of this variable for some uses (e.g. irrigation schedule) is also lower. Two factors seem to be relevant for wind speed estimation problems: i) the high spatial variability of wind speed Luo et al. (2008) and ii) the fact that wind speed is not normally distributed, while both gap filling and interpolation processes perform better with normally adjusted data.

20 These comparisons also detected some problems related with dewpoint temperature predicted values in summer. Inverse bias are detected between inland and maritime regions. In summer months, the humidity contrast between inland and maritime regions is high in the Iberian Peninsula, as maritime regions present higher humidity due to the contribution of sea breezes. The detected overestimation of dewpoint temperature in summer in continental regions leads to an underestimation of vapor pressure deficit and also to an underestimation of ET_o. Because of this effect, it is probable that some underestimation of ET_o
25 values is produced in the continental regions of Spain, while the maritime regions could be affected by an overestimation.

The performance of the homogenization process was also tested detecting changes in the spatial mean values of the first decades in some of the climatic variables. While maximum and minimum temperature are affected by an increase in their spatial mean, wind speed is affected by a decrease in the spatial mean. Due to counteracting effects, ET_o mean spatial value is not affected by this problem.

30 Considering that each estimation process is affected by an uncertainty, a methodology to obtain the uncertainty of ET_o after the two estimation processes was also implemented. For simplicity, independence between climatic variables was considered in the final step of the uncertainty estimation, which is the propagation of the uncertainty of each climatic variable through the Penman-Monteith equation.

While Haylock et al (2008) pointed out that variance of the kriging, which in this paper was used as the uncertainty of
35 each climatic grid, is not a true estimation of the uncertainty, the evaluation of the estimation of the uncertainty for each

variable showed a good accordance between MAE values and estimated uncertainty values. Unfortunately, the uncertainty of ET_o cannot be verified as an independent subset of observatories collecting all variables required to calculate ET_o was not available.

This dataset was firstly developed to generate, in combination with precipitaation data, drought climate grids for the study
5   area (Vicente-Serrano et al., 2017), but finally this ET_o climate grid is made available due to the high number of possible uses of this data. As with drought studies, in some cases, the interest is focused on the combined anaysis of ET_o and precipitation data.

This could be the case of hydrological studies, in which the AED data is relevant to explain some of the most important processes taking place in a catchment. Better estimations of ET_o should also lead to obtain better estimations of water balance
10   and aridity indices. As the presented dataset covers a long period, the temporal evolution of these indices could be studied.

Irrigated agriculture is another interested sector in these studies, as the water balance is important both for irrigation planning and also for irrigation schedule. Due to the development of modern irrigation systems, irrigation is a relevant economic activity at some regions in Spain, such as the Ebro basin (Vidal-Macua et al., 2018), which reinforces the importance of the presented dataset in the region. But not only the irrgated agriculture is interested in the study of ET_o. In general, the whole agricultural
15   sector is interested in a better knowledge of ET_o and/or ET_c (obtained multiplying ET_o by a crop coefficient - Kc)

For climatology, this dataset could also be interpreted as the first available AED climate grid in Spain, which is quite relevant to develop spatial and temporal studies to confirm the previously detected positive trends of this variable in the study area. This database could also be used to study the ability of distinct climate models (regional or global) to resolve the energy and water balance for an observed period, which is relevant for climate change studies, as a comparison of analysis and/or historical
20   experiments against observational data is necessary whenever climate models are evaluated for projected scenarios.

6   Data availability

The four files generated in this dataset (weekly values of reference evapotranspiration, uncertainty estimation of weekly values of reference evapotranspiration, aerodynamic component values of weekly reference evapotranspiration and radiative component values of weekly referenece evapotranspiration) can be accesed and downloaded via two different sources.
25   From Digital CSIC, which is a long-term repository managed by the Spanish Research Council (CSIC), users can download the files in netcdf format through http://dx.doi.org/10.20350/digitalCSIC/8615 (Tomas-Burguera et al., 2019)

The data can also be accessed in the web page http://speto.csic.es, which is a map visualization tool. Users can visualize the data for the different time steps available, download the complete netcdf files or download a complete time series for a chosen point as a comma-separated value (csv) file. As the spatial resolution of the data is 1.1 km for the Continental Spain
30   and Balearic Islands, the total number of grid points is slightly higher than 400.000. Due to the weekly temporal resolution, 2592 different weekly maps for each of the four files ara available

Author contributions. Miquel Tomas-Burguera, in collaboration with Sergio M. Vicente-Serrano and Santiago Beguería, conceived the research. Miquel Tomas-Burguera developed the quality control of the data, contributed to the computation of ET_o, developed the data validation and prepared the manuscript. Santiago Beguería developed methods for data reconstruction and climate mapping. Fergus Reig and Borja Latorre processed the data and developed the web portal infrastructure.

5 *Competing interests.* The authors declare no conflict of interest

7 Acknowledgements

This work was supported by research projects PCIN-2015-220, CGL2014-52135-C03-01, CGL2014-52135-C03-02, CGL2014-52135-C03-03 and CGL2017-83866-C3-3-R financed by the Spanish Commission of Science and Technology and FEDER. The work of M. Tomas-Burguera was supported by the predoctoral FPU program 2013 (Ministerio de Educación, Cultura y
10 Deporte). The authors thank the Spanish Meteorological Agency (AEMET) for providing the original data.

References

Aalto, J., Pirinen, P., Heikkinen, J., and Venäläinen, A.: Spatial interpolation of monthly climate data for Finland: Comparing the performance of kriging and generalized additive models, Theoretical and Applied Climatology, 112, 99–111, https://doi.org/10.1007/s00704-012-0716-9, 2013.

5 Alexandersson, H.: A homogeneity test applied to precipitation data, Journal of Climatology, 6, 661–675, https://doi.org/10.1002/joc.3370060607, https://doi.org/10.1002/joc.3370060607, 1986.

Allen, R. G., Pereira, L. S., Raes, D., and Smith, M.: FAO Irrigation and Drainage Paper Crop by, Irrigation and Drainage, 300, 300, https://doi.org/10.1016/j.eja.2010.12.001, http://www.kimberly.uidaho.edu/water/fao56/fao56.pdf, 1998.

Azorin-Molina, C., Vicente-Serrano, S. M., Mcvicar, T. R., Jerez, S., Sanchez-Lorenzo, A., López-Moreno, J. I., Revuelto, J., Trigo, R. M.,
10 Lopez-Bustins, J. A., and Espírito-Santo, F.: Homogenization and assessment of observed near-surface wind speed trends over Spain and Portugal, 1961-2011, Journal of Climate, 27, 3692–3712, https://doi.org/10.1175/JCLI-D-13-00652.1, 2014.

Azorin-Molina, C., Vicente-Serrano, S. M., Sanchez-Lorenzo, A., McVicar, T. R., Morán-Tejeda, E., Revuelto, J., El Kenawy, A., Martín-Hernández, N., and Tomas-Burguera, M.: Atmospheric evaporative demand observations, estimates and driving factors in Spain (1961-2011), Journal of Hydrology, 523, 262–277, https://doi.org/10.1016/j.jhydrol.2015.01.046, http://dx.doi.org/10.1016/j.jhydrol.2015.01.
15 046, 2015.

Beguería, S., Vicente-Serrano, S. M., Tomás-Burguera, M., and Maneta, M.: Bias in the variance of gridded data sets leads to misleading conclusions about changes in climate variability, International Journal of Climatology, 36, 3413–3422, https://doi.org/10.1002/joc.4561, 2016.

Beguería, S., Tomas-Burguera, M., Serrano-Notivoli, R., Peña-Angulo, D., Vicente-Serrano, S. M., and González-Hidalgo, J. C.: Gap filling
20 of monthly temperature data and its effect on climatic variability and trends, Submitted, 2019.

Cressie, N. A. C.: Statistics for Spatial Data, Wiley, New Yor, 1993.

del Río, S., Cano-Ortiz, A., Herrero, L., and Penas, A.: Recent trends in mean maximum and minimum air temperatures over Spain (1961-2006), Theoretical and Applied Climatology, 109, 605–626, https://doi.org/10.1007/s00704-012-0593-2, 2012.

Espadafor, M., Lorite, I. J., Gavilán, P., and Berengena, J.: An analysis of the tendency of reference evapotranspiration esti-
25 mates and other climate variables during the last 45 years in Southern Spain, Agricultural Water Management, 98, 1045–1061, https://doi.org/10.1016/j.agwat.2011.01.015, http://dx.doi.org/10.1016/j.agwat.2011.01.015, 2011.

Gonzalez-Hidalgo, J. C., Peña-Angulo, D., Brunetti, M., and Cortesi, N.: MOTEDAS: A new monthly temperature database for mainland Spain and the trend in temperature (1951-2010), International Journal of Climatology, 35, 4444–4463, https://doi.org/10.1002/joc.4298, 2015.

30 Gonzalez-Hidalgo, J. C., Peña-Angulo, D., Brunetti, M., and Cortesi, N.: Recent trend in temperature evolution in Spanish mainland (1951–2010): From warming to hiatus, International Journal of Climatology, 36, 2405–2416, https://doi.org/10.1002/joc.4519, 2016.

Gräler, B., Pebesma, E., and Heuvelink, G.: Spatio-temporal geostatistics using gstat, The R Journal, 8, 204–218, https://doi.org/10.1007/978-3-319-17885-1, http://edepot.wur.nl/427175, 2016.

Hargreaves, G. and Samani, Z.: Reference crop evapotranspiration from temperature, Applied Engineering in Agriculture, 1, 96–99, 1985.

35 Haslinger, K. and Bartsch, A.: Creating long-term gridded fields of reference evapotranspiration in Alpine terrain based on a recalibrated Hargreaves method, Hydrology and Earth System Sciences, 20, 1211–1223, https://doi.org/10.5194/hess-20-1211-2016, 2016.

Haylock, M. R., N. Hofstra, A.M.G. Klein Tank, E.J. Klok, P.D. Jones, and New., M.: A European daily high-resolution gridded dataset of surface temperature and precipitation, Journal of Geophysical Research-Atmospheres, 113, D20 119, https://doi.org/10.1029/2008JD010201, 2008.

Hofstra, N., Haylock, M., New, M., Jones, P., and Frei, C.: Comparison of six methods for the interpolation of daily, European climate data, Journal of Geophysical Research Atmospheres, 113, https://doi.org/10.1029/2008JD010100, 2008.

Irmak, S., Kabenge, I., Skaggs, K. E., and Mutiibwa, D.: Trend and magnitude of changes in climate variables and reference evapotranspiration over 116-yr period in the Platte River Basin, central Nebraska-USA, Journal of Hydrology, 420-421, 228–244, https://doi.org/10.1016/j.jhydrol.2011.12.006, http://dx.doi.org/10.1016/j.jhydrol.2011.12.006, 2012.

Luo, W., Taylor, M., and Parker, S.: A comparison of spatial interpolation methods to estimate continuous wind speed surfaces using irregularly distributed data from England and Wales, 28, 947–959, https://doi.org/10.1002/joc.1583, 2008.

Mardikis, M. G., Kalivas, D. P., and Kollias, V. J.: Comparison of interpolation methods for the prediction of reference evapotranspiration - An application in Greece, Water Resources Management, 19, 251–278, https://doi.org/10.1007/s11269-005-3179-2, 2005.

McVicar, T. R., Van Niel, T. G., Li, L. T., Hutchinson, M. F., Mu, X. M., and Liu, Z. H.: Spatially distributing monthly reference evapotranspiration and pan evaporation considering topographic influences, Journal of Hydrology, 338, 196–220, https://doi.org/10.1016/j.jhydrol.2007.02.018, 2007.

Mcvicar, T. R., Roderick, M. L., Donohue, R. J., and Van Niel, T. G.: Less bluster ahead? ecohydrological implications of global trends of terrestrial near-surface wind speeds, Ecohydrology, 5, 381–388, https://doi.org/10.1002/eco.1298, 2012.

Mendicino, G. and Senatore, A.: Regionalization of the Hargreaves Coefficient for the Assessment of Distributed Reference Evapotranspiration in Southern Italy, Journal of Irrigation and Drainage Engineering, 139, 349–362, https://doi.org/10.1061/(ASCE)IR.1943-4774.0000547, http://ascelibrary.org/doi/10.1061/{%}28ASCE{%}29IR.1943-4774.0000547, 2013.

Pebesma, E. J.: Multivariable geostatistics in S: The gstat package, Computers and Geosciences, 30, 683–691, https://doi.org/10.1016/j.cageo.2004.03.012, 2004.

Robinson, E. L., Blyth, E. M., Clark, D. B., Finch, J., and Rudd, A. C.: Trends in atmospheric evaporative demand in Great Britain using high-resolution meteorological data, Hydrology and Earth System Sciences, 21, 1189–1224, https://doi.org/10.5194/hess-21-1189-2017, 2017.

Samani, Z.: Estimating solar radiation and evapotranspiration using minimum climatological data, Journal of Irrigation and Drainage Engineering, 126, 265–267, 2000.

Sanchez-Lorenzo, A., Calbó, J., and Wild, M.: Global and diffuse solar radiation in Spain: Building a homogeneous dataset and assessing their trends, Global and Planetary Change, 100, 343–352, https://doi.org/10.1016/j.gloplacha.2012.11.010, http://dx.doi.org/10.1016/j.gloplacha.2012.11.010, 2013.

Sanchez-Lorenzo, A., Vicente-Serrano, S. M., Wild, M., Calbó, J., Azorin-Molina, C., and Peñuelas, J.: Evaporation trends in Spain: A comparison of class A pan and Piché atmometer measurements, Climate Research, 61, 269–280, https://doi.org/10.3354/cr01255, 2014.

Sheffield, J., Wood, E. F., and Roderick, M. L.: Little change in global drought over the past 60 years, Nature, 491, 435–438, https://doi.org/10.1038/nature11575, http://dx.doi.org/10.1038/nature11575, 2012.

Thornthwaite, C. W.: An Approach toward a Rational Classification of Climate, Geographical Review, 38, 55, https://doi.org/10.2307/210739, http://www.jstor.org/stable/210739?origin=crossref, 1948.

Tomas-Burguera, M., Jiménez Castañeda, A., Luna Rico, M. Y., Morata, A., Vicente-Serrano, S., González-Hidalgo, J. C., and Beguería, S.: Control de calidad de siete variables del banco nacional de datos de AEMET, in: X Congreso Internacional AEC: Clima, sociedad, riesgos y ordenación del territorio, edited by Olcina Cantos, J., Rico Amorós, A. M., and Moltó Manterio, E., pp. 407–415, Alicante, 2016.

Tomas-Burguera, M., Vicente-Serrano, S. M., Grimalt, M., and Beguería, S.: Accuracy of reference evapotranspiration (ETo) estimates under data scarcity scenarios in the Iberian Peninsula, Agricultural Water Management, 182, 103–116, https://doi.org/10.1016/j.agwat.2016.12.013, http://dx.doi.org/10.1016/j.agwat.2016.12.013, 2017.

Tomas-Burguera, M., Beguería, S., Vicente-Serrano, S. M., Reig, F., and Latorre, B.: SPETo (Spanish reference evapotranspiration) [Dataset], https://doi.org/http://dx.doi.org/10.20350/digitalCSIC/8615, 2019.

Vanderlinden, K., Giráldez, J. V., and Van Meirvenne, M.: Assessing Reference Evapotranspiration by the Hargreaves Method in Southern Spain, Journal of Irrigation and Drainage Engineering, 130, 184–191, https://doi.org/10.1061/(asce)0733-9437(2004)130:3(184), 2004.

Vicente-Serrano, S. M., Azorin-Molina, C., Sanchez-Lorenzo, A., Revuelto, J., López-Moreno, J. I., González-Hidalgo, J. C., Moran-Tejeda, E., and Espejo, F.: Reference evapotranspiration variability and trends in Spain, 1961-2011, Global and Planetary Change, 121, 26–40, https://doi.org/10.1016/j.gloplacha.2014.06.005, http://dx.doi.org/10.1016/j.gloplacha.2014.06.005, 2014.

Vicente-Serrano, S. M., Tomas-Burguera, M., Beguería, S., Reig, F., Latorre, B., Peña-Gallardo, M., Luna, M. Y., Morata, A., and González-Hidalgo, J. C.: A High Resolution Dataset of Drought Indices for Spain, Data, 2, 22, https://doi.org/10.3390/data2030022, http://www.mdpi.com/2306-5729/2/3/22, 2017.

Vidal-Macua, J. J., Ninyerola, M., Zabala, A., Domingo-Marimon, C., Gonzalez-Guerrero, O., and Pons, X.: Environmental and socioeconomic factors of abandonment of rainfed and irrigated crops in northeast Spain, Applied Geography, 90, 155–174, https://doi.org/10.1016/j.apgeog.2017.12.005, https://doi.org/10.1016/j.apgeog.2017.12.005, 2018.
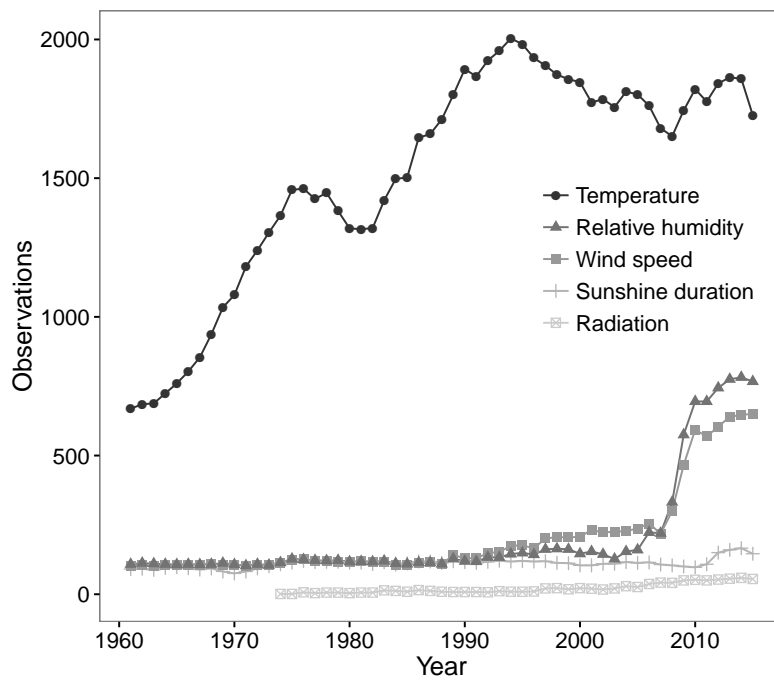
Figure 1. Temporal evolution of data availability.

Interpolation   ETo calculation
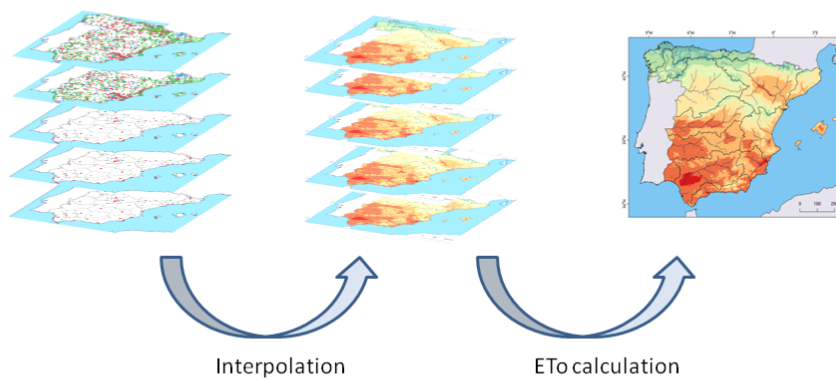
Figure 2. Main steps in the generation of ET$_o$ database. First we interpolate each climatic variable and then we calculate ET$_o$.
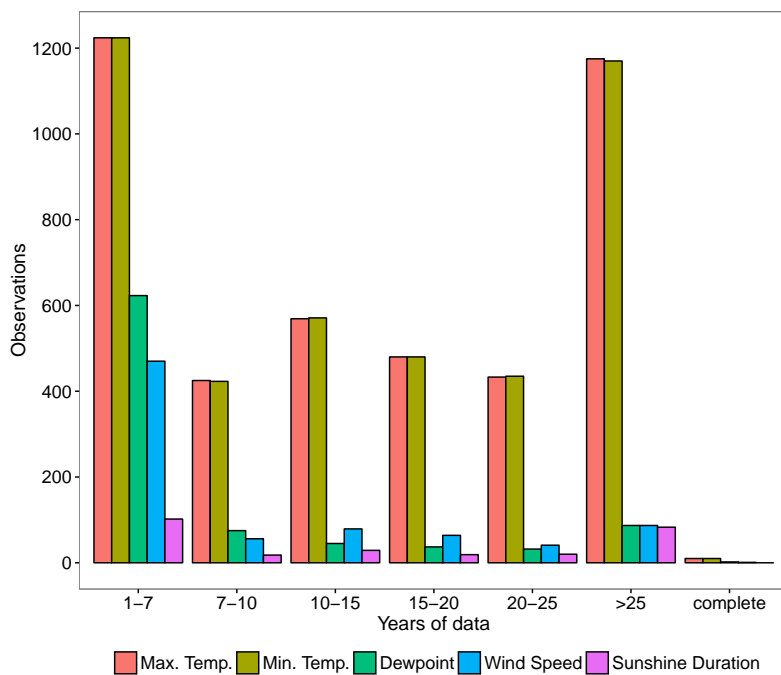
Figure 3. Number of available observations grouped by variables and by years of data available.
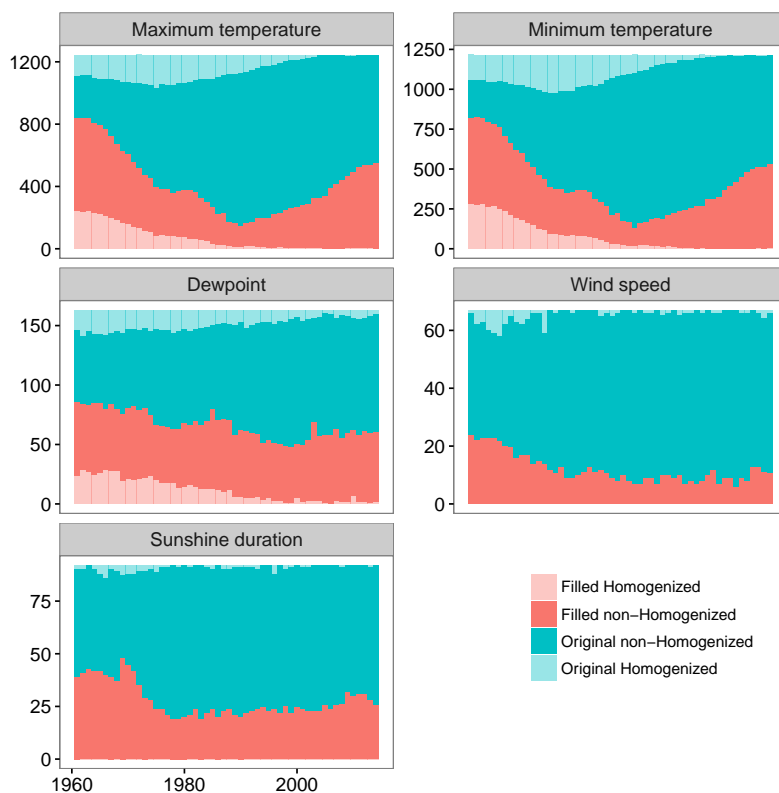
Figure 4. Temporal evolution of the number of filled data for the different climatic variables. The temporal evolution of homogenized data is also shown.
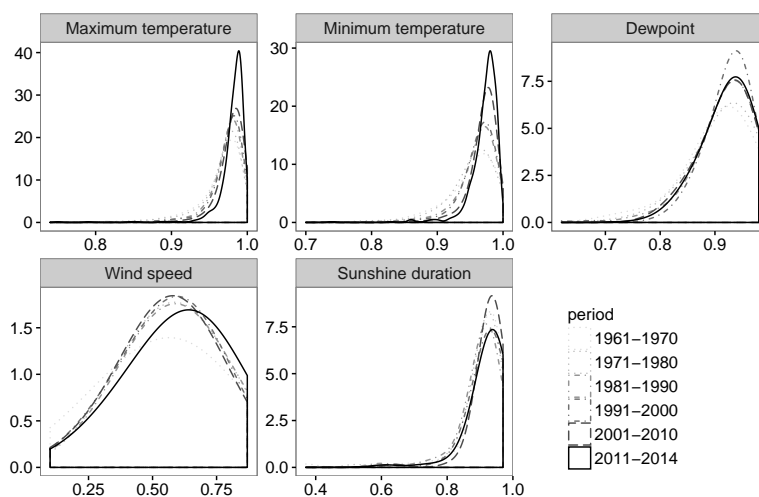
Figure 5. Kernel density of gap filling R^2 grouped by decadal periods.
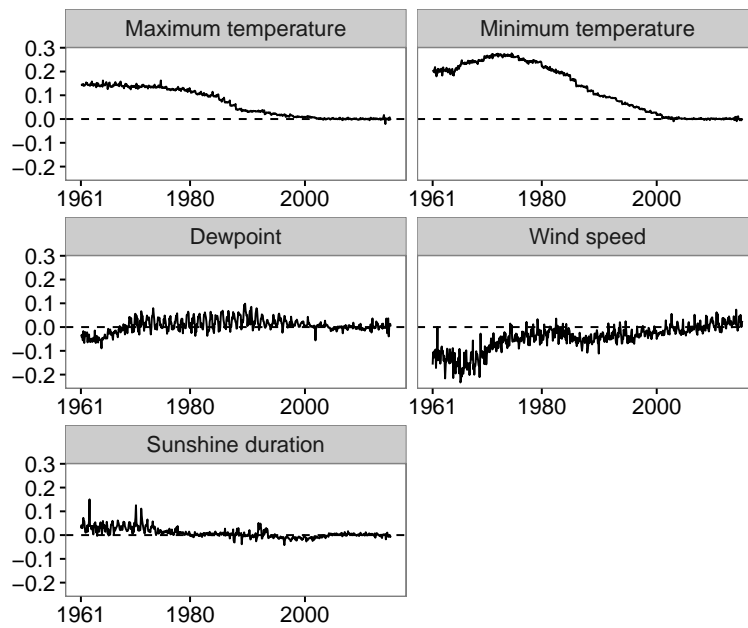
Figure 6. Temporal evolution of differences between mean regional values before and after the homogenization.
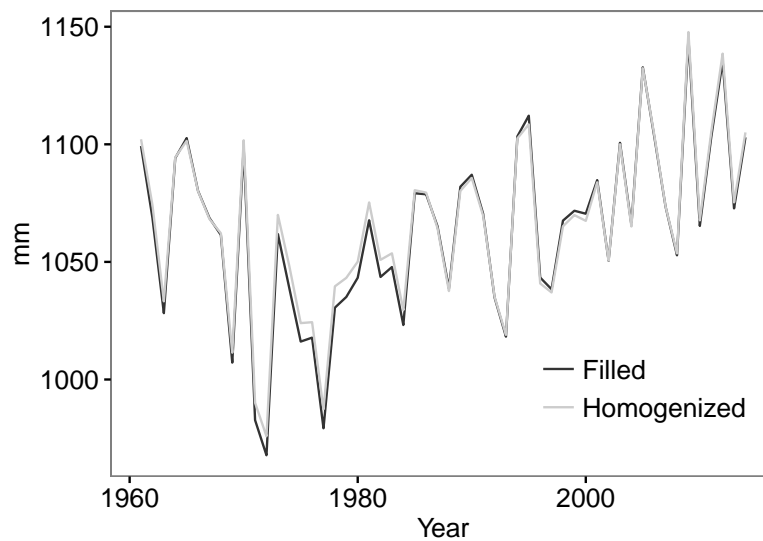
Figure 7. Temporal evolution of mean regional values of ET_o between mean regional values before (Filled) and after (Homogenized) the homogenization.
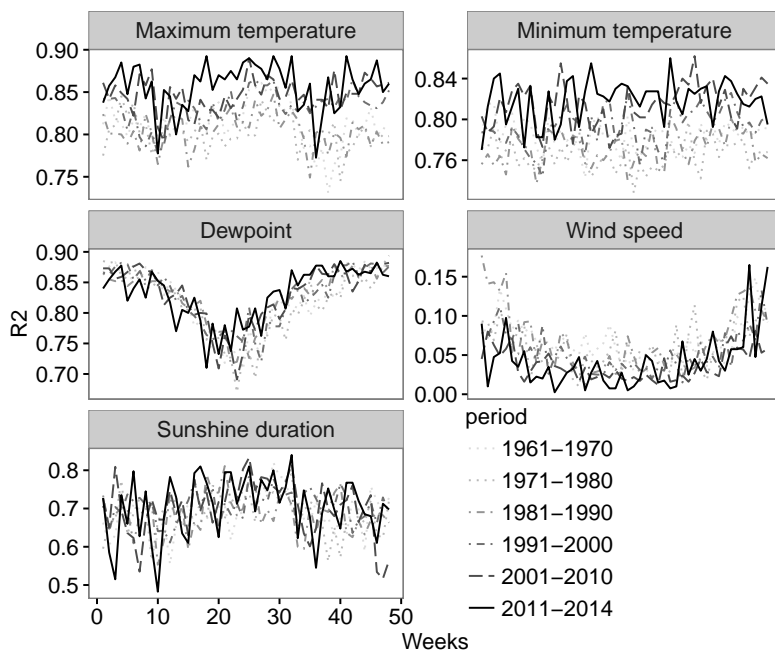
Figure 8. Spatial validation of interpolation in terms of R^2 grouped by decadal periods.
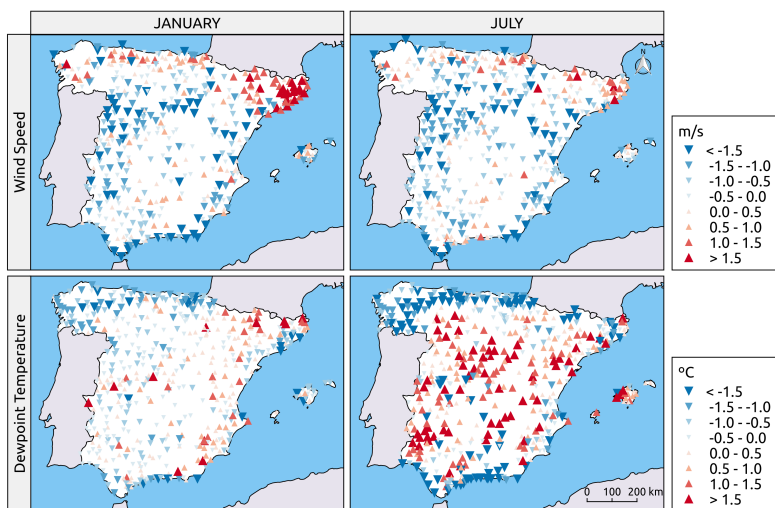
Figure 9. Spatial validation of dewpoint and wind speed climatic grids by using a subset of independent observations for the 2010-2014 period in terms of Mean Error.
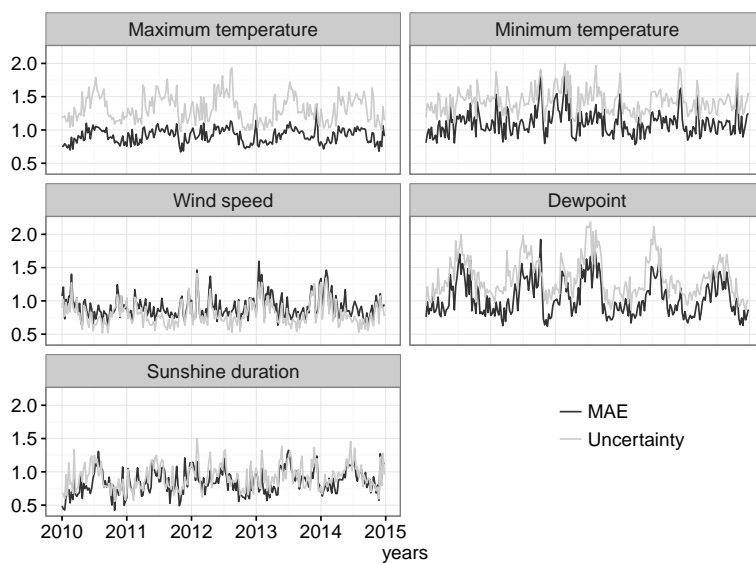
Figure 10. Temporal evolution of MAE and uncertainty of interpolation at a subset of independent observations for the 2010-2014 period.
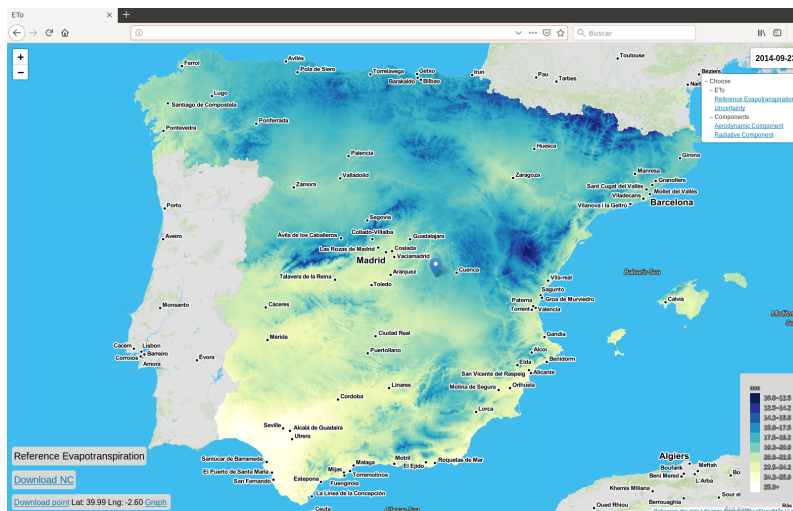
Figure 11. Example of the data visualitzation in the web page http://speto.csic.es.

Table 1. Number of weather stations per variable

Variable	Weather stations	
	Available	Selected
Maximum temperature	4306	1246
Minimum temperature	4303	1217
Relative humidity	899	164
Wind speed	797	67
Sunshine duration	271	92

Table 2. Comparison of the number of weather stations used to generate the climate dataset and the number of observations available during 2010-2014 period.

Variable	Original database	2010-2014
Maximum temperature	1246	1186
Minimum temperature	1217	1195
Relative humidity	164	648
Wind speed	67	583
Sunshine duration	92	80

Table 3. Gap filling performance

Variable	MAE	R^2	ME	PBIAS	rM	rSD
Maximum temperature (℃)	0.92	0.97	0.00	0.00	0.99	1.00
Minimum temperature (℃)	0.83	0.95	0.00	0.00	0.99	1.00
Dewpoint temperature (℃)	1.04	0.91	-0.01	-0.15	0.99	1.00
Sunshine duration (h)	0.63	0.91	-0.01	-0.23	0.99	1.00
Wind speed (kmh^{-1})	2.32	0.53	0.08	0.64	1.00	1.05

Table 4. Percentage of data affected by inhomogeneities.

	Weekly data	Original data	Filled data
Maximum temperature (℃)	14,8 %	13,7 %	17 %
Minimum temperature (℃)	16,7 %	14,8 %	20,3 %
Dewpoint temperature (℃)	14,1 %	11,2 %	18,2 %
Wind speed (ms^{-1})	3,1 %	1,8 %	8,9 %
Sunshine duration (h)	10,1 %	7,2 %	16,8 %

Table 5. Spatial and temporal validation of interpolation

Variable	Validation	MAE	R^2	ME	PBIAS	rM	rSD
Maximum temperature (℃)	Temporal	1.02	0.98	-0.02	0.00	0.99	0.99
	Spatial	1.02	0.82	-0.02	0.00	0.99	0.92
Minimum temperature (℃)	Temporal	1.11	0.97	0.03	0.01	1.00	0.98
	Spatial	1.11	0.78	0.04	0.00	1.00	0.89
Dewpoint temperature (℃)	Temporal	1.01	0.95	0.05	0.02	1.00	0.98
	Spatial	1.02	0.82	0.06	0.00	0.99	0.89
Sunshine duration (h)	Temporal	0.65	0.93	0.00	0.48	1.00	0.97
	Spatial	0.64	0.70	0.00	0.12	1.00	0.85
Wind speed (ms^{-1})	Temporal	0.75	0.54	0.05	12.31	1.12	0.87
	Spatial	0.75	0.06	0.06	2.44	1.02	0.46